THE ASTROPHYSICAL JOURNAL, 401:L83–L86, 1992 December 20

THE ULTRAVIOLET COLOR GRADIENT IN THE LATE-TYPE SPIRAL GALAXY M33

WAYNE B. LANDSMAN,[1] MORTON S. ROBERTS,[2] RALPH C. BOHLIN,[3] ROBERT W. O'CONNELL,[4]
ANDREW M. SMITH,[5] AND THEODORE P. STECHER[5]
Received 1992 July 6; accepted 1992 October 5

ABSTRACT

The ultraviolet surface brightness and color distributions for the late-type spiral galaxy M33 are derived from images at 1520 and 2490 Å that were obtained by the Ultraviolet Imaging Telescope (UIT) on the Astro Spacelab mission. Although the surface brightness shows a general decline with radius, the dominant spiral arms cause significant deviations from an exponential fit. Colors in elliptical annuli become 0.2–0.3 mag bluer with increasing radius. Our measures of individual H II regions and sections of spiral arms follow this same trend. Interarm regions are redder than the arms. A metallicity gradient affecting only the colors of stars is inadequate in accounting for the observed color gradient. A plausible explanation invokes a combination of an LMC-type reddening curve and a radial gradient in the internal reddening in M33.

Subject headings: galaxies: individual (M33) — galaxies: photometry — ultraviolet: galaxies

1. INTRODUCTION

Ultraviolet images of M33 were obtained with the ASTRO/UIT experiment flown aboard the Shuttle Columbia in 1990 December. M33 is the nearest Sc-type galaxy and is a prominent member of the Local Group. Its large angular diameter makes it well suited to the UIT 40′ field. Details regarding the UIT experiment are given in Stecher et al. (1992).

Ultraviolet imaging enhances the hot stellar population while suppressing the cooler stars. In the case of M33 where the familiar blue and visual images show prominent bulky arms superposed on a cool-disk population, the change is striking. In the ultraviolet, the dominant arms appear as extended clumps of pointlike and nebulous features. These hot stars in H II regions and stellar OB associations outline the more familiar arms. We present here some of the UV images together with several quantitative results derived from these images, e.g., the UV surface brightness and color profiles.

2. OBSERVATIONS

A total of 11 images of M33 were recorded on 70 mm IIa-0 roll film and obtained with differing exposure times and with four different filter-detector combinations. The images of M33 were offset from the nucleus so that the Hopkins experiment (HUT) could obtain spectra of the bright M33 H II region NGC 595 while the UIT frames were being exposed. Two images with the longest exposures are discussed here, a far-UV frame (number 496) of 424 s and a near-UV exposure (number 402) of 416 s. These images have effective wavelengths of 1520 Å (FUV filter B1 with bandpass of 354 Å) and 2490 Å (NUV filter A1 with bandpass of 1150 Å) and are shown in Figure 1 (Plate L7) along with ground-based V and Hα images. The resolution of the UIT images is $\sim 3''$.

The positions of 146 sources found in common on the FUV and NUV images were used to correct for geometric distortions in the UIT images. A mean residual of 2.″7 between the source positions remained following the warping correction. Several image defects are patched over; these include scratches introduced during the film processing, and "turn-on spots" of decreased sensitivity that are caused by the slow development of uniform charge on the photocathode following the turn-on of the high voltage. Most Galactic foreground stars are too cool to appear on the UV images; but 30 stars on the NUV image and two stars (SAO 54780 and an A-type star near NGC 604) on the FUV image were patched over prior to the surface photometry.

The magnitudes, m_λ, given in this *Letter* are defined as $-2.5 \times \log f_\lambda - 21.1$, where f_λ is the mean flux in the A1 or B1 filter in ergs cm^{-2} s^{-1} Å^{-1}.

3. COLOR GRADIENTS

3.1. *The Surface Brightness and Color Distributions*

Fluxes measured within elliptical annuli are shown for both the FUV and NUV frames in Figure 2. These data are not corrected for extinction, either foreground or internal to M33. The annuli of width 48″ are centered on the nucleus and have a position angle of 23° and an axial ratio of 1.6 (van den Bergh 1991). As the annuli size increases, one part reaches the edge of the frame. Measurements are continued using partial annuli; thus at $R = 13.'2$, the fractional area of the usable part of the annulus is 97%, while at $R = 19.'6$, only 39% of the galaxy is in the field of view. An asymmetry in the light or color of M33 could distort the data for $R > 14'$; in particular, the UIT images do not include the bright H II region 250–251 from the catalog of Boulesteix et al. (1974).

Both the FUV and NUV surface brightness distributions show a steep decline over the inner 3′, followed by a more gradual decrease at larger radii. The presence of bright H II regions (note especially NGC 604 at $R = 14.'4$) causes the surface brightness distribution to deviate from an exponential. However, an exponential scale length can be determined by taking the median value of the fluxes within each annulus. The scale length is determined this way to be 5.′6 at 2490 Å and 7.′0 at 1520 Å.

[1] Hughes/STX, Code 681, NASA/GSFC, Greenbelt, MD 20771.
[2] National Radio Astronomy Observatories, 520 Edgemont Road, Charlottesville, VA 22903. Operated by Associated Universities, Inc. under Cooperative Agreement with the National Science Foundation.
[3] Space Telescope Science Institute, Baltimore, MD 21218.
[4] University of Virginia, Astronomy Department, P.O. Box 3818, Charlottesville, VA 22903.
[5] Laboratory for Astronomy and Solar Physics, Code 680, NASA/GSFC, Greenbelt, MD 20771.

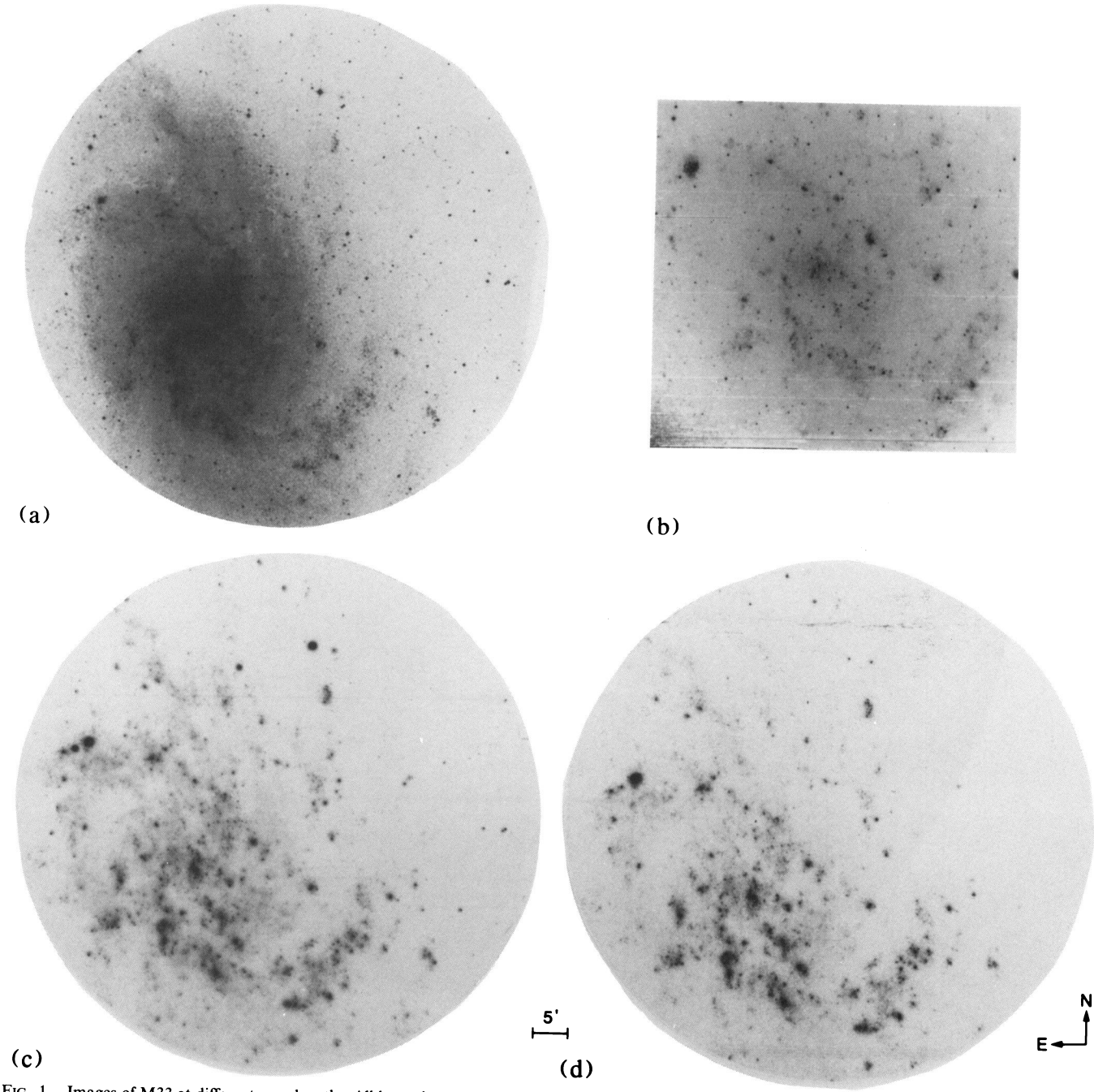

FIG. 1.—Images of M33 at different wavelengths. All have the same scale and orientation. (*a*) The *HST* Guide Star Catalog *V*-band image taken with the 1.2 m Palomar Schmidt. (*b*) An Hα image taken with the 0.9 m Kitt Peak Telescope and made available by R. Green and G. Jacoby. (*c*) The UIT near-UV image, $\lambda_{\rm eff} = 2490$ Å, $\Delta\lambda = 1150$ Å. (*d*) The UIT far-UV image, $\lambda_{\rm eff} = 1520$ Å, $\Delta\lambda = 354$ Å. The UIT fields are 40′ in diameter.

LANDSMAN et al. (see 401, L83)

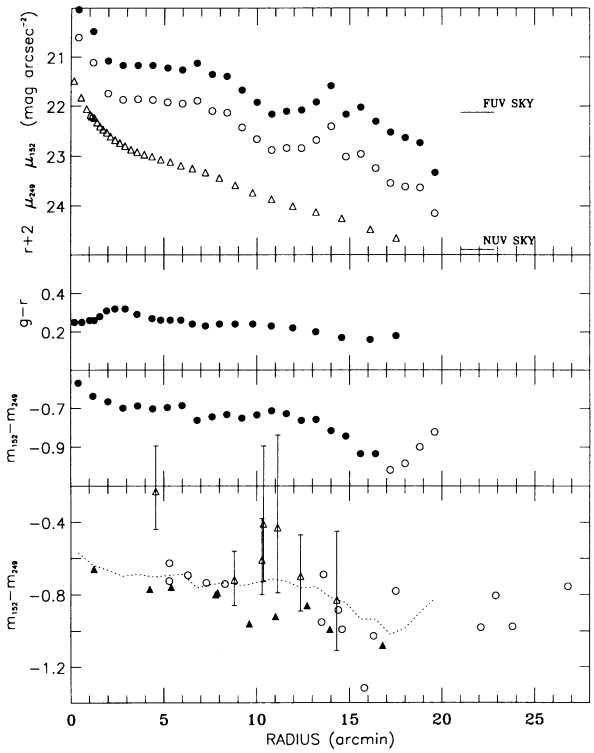

FIG. 2.—The surface brightness distribution of M33 measured in specific regions. *Upper panel:* in confocal ellipses for FUV 496 (1520 Å) (*filled circles*); NUV 402 (2490 Å) (*open circles*); *r*-band photometry from Kent 1987 (*open triangles* with a +2 mag offset for clarity. *Second panel:* colors in magnitudes for the same confocal ellipses as the top panel in $g - r$. *Third panel:* colors for the same confocal ellipses as the top panel for the UIT UV bands. The four open circles are colors from annuli which are not completely contained in the UIT field of view. *Bottom panel:* the dashed line is the same data as the points in the third panel, while the open circles are the UV colors of selected H II regions from Table 1. The triangles are the UV colors of the arm (*filled*) and interarm (*open*) regions that are displayed in Fig. 3. Despite the large error bars, the faint interarm regions as a group are significantly redder than the spiral arms or typical H II region.

The accuracy of the absolute calibration of the UIT photometry is estimated at 15% for each filter. In addition to this systematic uncertainty, various statistical uncertainties are also present. For example, the use of a background from a remote location on the film limits the precision of low surface brightness measurements because of the fundamental variation in the background fog level. Such background variations cause uncertainties in the colors $m_{152} - m_{249}$ of 5% at $R \sim 12'$ and 10% at $R \sim 18'$. Therefore, the drop in color from -0.7 in the inner parts to -0.9 in the 15′–18′ radius range of Figure 2 is measured with about a 2 σ uncertainty.

The surface brightness curve as measured in the near-red ($\sim$6500 Å) by Kent (1987) is also shown in Figure 2. Similar curves for 12 μm and 100 μm are given in Rice et al. (1990, Fig. 4). The distribution of H I (Deul & van der Hulst 1987, Fig. 10), the principal cool gas component, can be approximated by two horizontal lines: for $0 < R < 6'$, $n(\mathrm{H\ I}) \sim 0.6 \times 10^{21}$ atoms cm^{-2}, for $6' < R \leq 27'$, $n(\mathrm{H\ I}) \sim 1.0 \times 10^{21}$ atoms cm^{-2}.

The central ($r \leq 3'$) "feature" in both surface brightness and color has been observed at other wavelengths and is the basis for the suggestion that M33 may have a small nuclear bulge (see van den Bergh 1991 for a summary). Such a bulge would be unusual, since the feature corresponds in color to a late-B spectral type. Rather, and in keeping with Kent's (1987) observation "that this region is still dominated by the spiral structure of the disk," we suggest that what we and others have seen is just a part of a spiral arm near the center of M33.

3.2. H II *Regions*

The integrated UIT fluxes of 16 bright, isolated, H II regions are given in Table 1. Flux measurements of the giant H II regions has not been possible with previous UV instrumentation, because the 10″ × 20″ aperture on *IUE* is matched only to the smaller H II regions in M33, while the 2.′5 aperture on the *ANS* satellite included flux from neighboring sources.

Archival *IUE* spectra available for four of the H II regions are convolved through the UIT filter curves to obtain the magnitudes given in the footnotes to Table 1. For the compact H II regions IC 131 and IC 132, there is good agreement between the UIT and *IUE* fluxes. The *IUE* aperture includes only a fraction of the UV flux from the giant H II regions NGC 604 and NGC 588, and in both cases the UV color measured with *IUE* is bluer than the global color measured with UIT. This color difference is probably due to the large-scale inhomogeneities in these nebulae (Hunter & Gallagher 1985).

Mas-Hesse & Kunth (1991) have computed the ratio, B, of the number of ionizing photons, N_{LyC} to the UV luminosity for numerous population synthesis models. They find B to have a modest dependence on the duration of star formation, the assumed upper mass limit and the slope of the initial mass function, and a strong dependence on the assumed UV extinction. We have computed similar synthesis models using the solar metallicity evolutionary tracks of Schaller et al. (1992), and the model atmospheres of Kurucz (1992). For a Salpeter

TABLE 1

UV FLUXES OF M33 H II REGIONS

Identification[a]	R	Diameter[b]	m_{152}[c]	m_{249}[c]
B77	5.′3	45″	12.86	13.49
B10	5.3	52	12.64	13.37
IC 142	6.3	45	12.97	13.67
NGC 595	7.3	68	11.88	12.61
B208	8.3	43	13.87	14.61
B691	13.5	47	13.02	13.98
NGC 592	13.6	60	12.01	12.70
NGC 604[d,e]	14.4	51 × 45	9.76	10.64
B734–735	14.6	47	12.85	13.84
B663–664	15.8	52	13.16	14.48
B749	16.3	47	12.83	13.86
IC 131[f]	17.5	43	12.98	13.76
B274	22.1	50	12.89	13.87
NGC 588[g]	22.9	50	12.34	13.15
IC 133	23.8	52 × 97	11.51	12.49
IC 132[h]	26.8	52	13.39	14.14

[a] H II region names from Boulesteix 1974 if NGC or IC names do not exist.

[b] Fluxes measured within a circle of specified diameter or rectangle of specified sides.

[c] Magnitudes are uncorrected for extinction.

[d] UIT fluxes measured on 16.8 s A1 image and 85.9 s B1 image. NGC 604 is saturated on the primary deep images.

[e] From *IUE* (SWP 7349 + LWR 6341), $m_{152} = 10.64$, $m_{249} = 11.97$.

[f] From *IUE* (SWP 14313 + LWR 10945), $m_{152} = 13.20$, $m_{249} = 13.85$.

[g] From *IUE* (SWP 10273 + LWR 8943), $m_{152} = 12.49$, $m_{249} = 13.74$.

[h] From *IUE* (SWP 9780 + LWR 8497), $m_{152} = 13.47$, $m_{249} = 14.21$.

initial mass function with an upper mass of 100 $M_\odot$, and assuming a duration of star formation of 5 Myr, and a foreground reddening of $E(B-V) = 0.07$ (van den Bergh 1991), we find $(\log N_{LyC})/L_{1520} = 13.47$. Using the Hα-derived Lyman-continuum luminosity of NGC 604 ($\log N_{LyC} = 51.5$) and NGC 595 ($\log N_{LyC} = 51.2$) given by Kennicutt (1984), and assuming the average LMC extinction curve of Fitzpatrick (1986) for the internal reddening, we derive a mean internal extinction toward NGC 604 of $E(B-V) = 0.17$ and toward NGC 595 of $E(B-V) = 0.30$. These extinction values are about one-half of those tabulated by Kennicutt from the ratio of radio continuum to Hα emission.

In general, the UIT images correlate well with the Hα image of M33, but there are some notable exceptions. The second brightest H II region in the ultraviolet listed in Table 1 is the IC 133 complex, but its Hα and H_2 emission are relatively weak, which Israel et al. (1990) attribute to an unusually small amount of gas and dust in the nebula. The OB association HS 142, located about 1′ south of the nucleus, is also bright on the UV image but weak in Hα. This association is known to lie in the direction of an H I "hole," number 81 in the catalog of Deul & den Hartog (1990), which is a feature 1′ in diameter. A more detailed comparison of the UV and Hα emission in M33 is deferred to a subsequent paper.

3.3. *Arm and Interarm Regions*

The regions in Figure 3 (Plate L8) enclose 17 of the most prominent localized maxima and minima of UV surface brightness. Table 2 contains the mean distance from the center of M33, the area, and the average surface brightness for each of these 17 regions of interest, while the bottom panel of Figure 2 shows the color of the 10 arm and seven interarm regions as a function of the mean distance from the center.

The colors in the interarm regions are difficult to measure, because the net signal is comparable to the sky background in the FUV and is only a few times the sky in the NUV. The errors on the colors of the seven faint interarm regions that appear in Figure 2 are dominated by a 17% uncertainty in the FUV sky level. The uncertainties in the brighter arm regions are typically 10 times smaller. The colors $m_{152} - m_{249}$ of the arm regions are bluer than the global averages for the entire galaxy in the confocal ellipses by an average of about 0.1 mag and follow the general trend with radius of the colors of the global averages and the H II regions. The colors of the interarm regions tend to lie above the average global colors by an amount that is not usually significant for an individual region; but taken as a whole, the interarms are definitely redder than the arms. However, the colors of the interarm regions are still bluer than observed in the disk of M81 ($m_{152} - m_{249} \sim 0.0$; Hill et al. 1992), suggesting a contribution from either a hot star component or from dust scattering of the UV emission in the arms.

TABLE 2

UV Surface Brightness of Arm and Interarm Regions

N	Type[a]	R	A (arcsec^2)	μ_{152}[b]	μ_{249}[b]
1.....	I	10.4	20341	22.86	23.28
2.....	A	9.6	10915	20.49	21.44
3.....	I	12.4	21912	22.23	22.93
4.....	A	12.7	14904	20.77	21.64
5.....	I	10.3	13767	22.25	22.86
6.....	A	5.4	8393	20.52	21.28
7.....	A	7.9	17529	20.23	21.02
8.....	A	7.8	21457	20.51	21.32
9.....	A	1.3	14553	20.19	20.85
10.....	A	4.3	23028	20.64	21.41
11.....	I	4.6	10977	22.34	22.57
12.....	I	11.1	73570	23.00	23.44
13.....	I	8.8	41322	21.87	22.59
14.....	A	11.0	10832	21.08	22.01
15.....	A	14.0	10315	20.55	21.54
16.....	I	14.3	26687	22.73	23.56
17.....	A	16.8	26604	20.82	21.89

[a] Arm (A) or interarm (I) region.

[b] Surface brightness in mag arcsec^{-2} uncorrected for extinction.

4. DISCUSSION

The UIT images of M33 show a UV color gradient in the global surface photometry, in the fluxes of individual H II regions, and in the fluxes of selected arm and interarm regions. The three data sets are somewhat independent since the H II region measurements employ a local background and are less subject to possible large scale background variations. Earlier observations of M33 with *OAO 2* (Davis et al. 1982), *ANS* (Israel, de Boer, & Bosma 1986), and *IUE* (Rosa, Joubert, & Benvenuti 1984) are consistent with the UV color gradient found here. A metallicity gradient is well established in M33 (Vílchez et al. 1987), and the $m_{152} - m_{249}$ color of hot stars is expected to become bluer with decreasing metallicity. However, the models of Kurucz (1992) suggest that the $m_{152} - m_{249}$ color would decrease by only ~0.12 for a factor of 10 decrease from solar metallicity.

Synthetic young star cluster spectra such as those discussed in § 3.2 generally give a $m_{152} - m_{249}$ color of ~ -1.3 for a zero-age burst and ~ -1.0 for a constant star formation model. These values are fairly insensitive to details of the star cluster model so long as the cluster is dominated by hot OB stars (which must exist in the H II regions). These model colors suggest that the UV color gradient could be due to a radial gradient in the proportion of past to current star formation. However, the star formation histories of the inner and outer H II regions must differ quite markedly to explain the entire UV color gradient.

An alternative explanation for the UV color gradient is a radial gradient in the internal reddening. We assume that the UV reddening properties in M33 are best represented by a LMC extinction curve (e.g., Bianchi, Hutchings, & Massey 1991), although the evidence is not yet conclusive. For the average Galactic curve of Cardelli, Clayton, & Mathis (1989), $E(m_{152} - m_{249}) \sim 0.7 \times E(B-V)$ while for the average LMC curve of Fitzpatrick (1986), $E(m_{152} - m_{249}) \sim 1.4 \times E(B-V)$. An intrinsic color $m_{152} - m_{249} = -1.15$ for the M33 OB associations and a Galactic foreground reddening of $E(B-V) = 0.07$, produces the observed UV color gradient in Figure 2 if the internal reddening is $E(B-V) \sim 0.27$ near the center of M33 and falls to $E(B-V) \sim 0.1$ at a radius of 13′. This result is consistent with the study of Wilson, Freedman, & Madore (1990), who found an internal extinction of $E(B-V) \sim 0.2$ from stellar photometry of three fields within 6′ of the nucleus of M33 and $E(B-V) \sim 0.1$ in a field at an (inclination-corrected) distance of ~22′ from the nucleus. This radial gradient in the internal reddening is likely related to the radial decrease in the dust-to-gas ratio determined from a comparison of the *IRAS* and H I maps of M33 (Rice et al. 1990; Deul 1989).

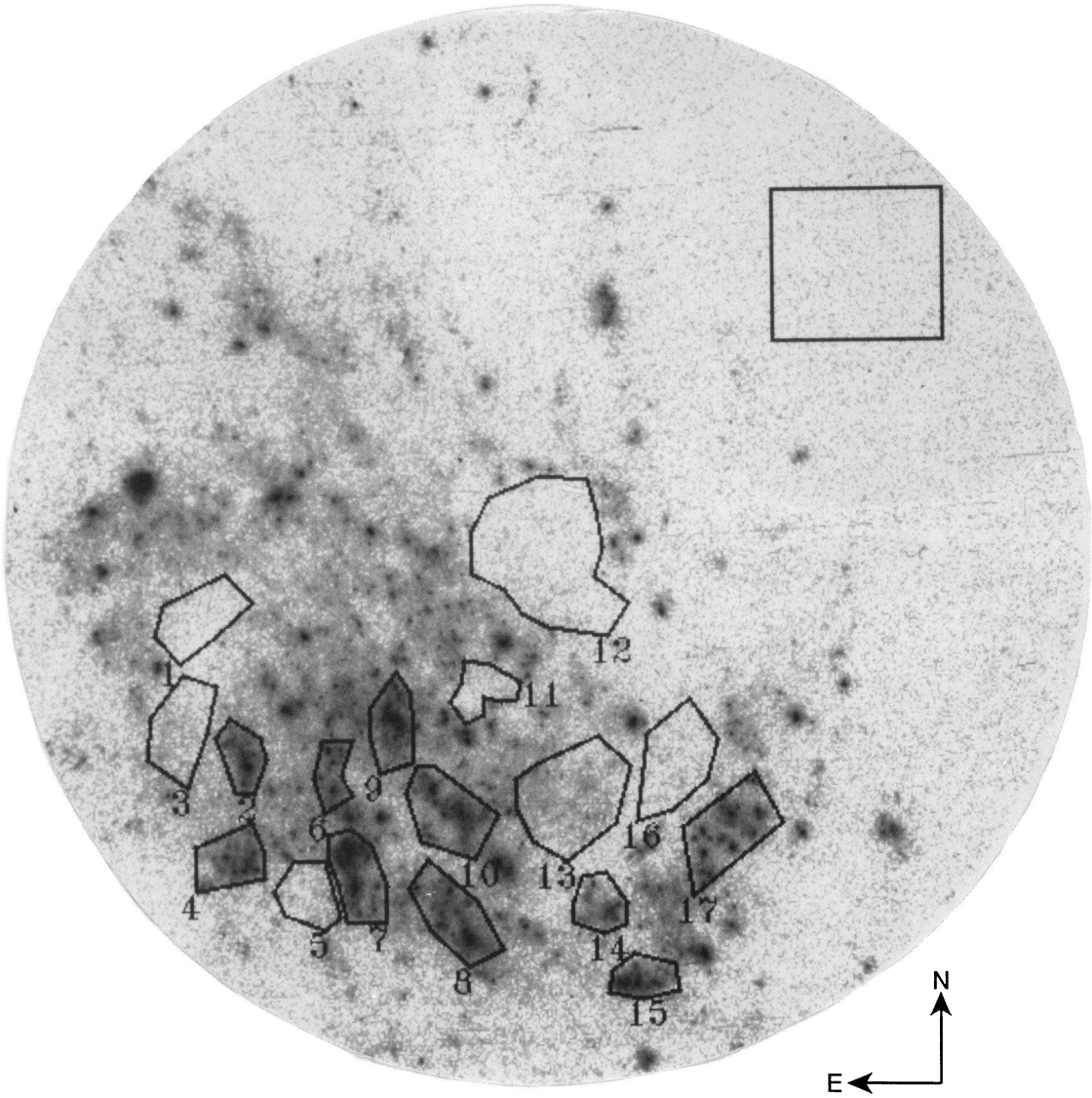

FIG. 3.—FUV 496 1520 Å image with the selected regions of Table 2 identified. The large square to the NW side of the image is the region used to define the sky background level. The center of the image is at $1^h33^m25^s.5$ and 30°44′06″ (J2000).

LANDSMAN et al. (see 401, L85)

In future work, we will present a more detailed comparison of the UV images with optical and radio data.

We are pleased to acknowledge the many people involved with the *Astro-1* mission who made these observations possible. We thank J van der Hulst for providing a copy of the 21 cm data and W. Waller and an anonymous referee for their comments on the manuscript. Funding for the UIT project has been through the Spacelab Office at NASA Headquarters under project number 440-41.

REFERENCES

Bianchi, L., Hutchings, J. B., & Massey, P. 1991, A&A, 249, 14
Boulesteix, J., Courtes, G., Laval, A., & Petit, H. 1974, A&A, 37, 33
Cardelli, J., Clayton, J., & Mathis, J. 1989, ApJ, 345, 245
Davis, J., Code, A. D., Mathis, J. S., & Welch, G. A. 1982, AJ, 87, 849
Deul, E. R. 1989, A&A, 218, 78
Deul, E. R., & den Hartog, R. H. 1990, A&A, 229, 362
Deul, E. R., & van der Hulst, J. M. 1987, A&AS, 67, 509
Fitzpatrick, E. L. 1986, AJ, 92, 1068
Hill, J. K., et al. 1992, ApJ, 395, L33
Hunter, D. A., & Gallagher, J. S. 1985, AJ, 90, 80
Israel, F. P., de Boer, K. S., & Bosma, A. 1986, A&AS, 66, 117
Israel, F. P., Hawarden, T. G., Geballe, T. R., & Wade, R. 1990, MNRAS, 242, 471
Kennicutt, R. C. 1984, ApJ, 287, 116
Kent, S. M. 1987, AJ, 94, 306
Kurucz, R. L. 1992, in The Stellar Populations of Galaxies, ed. B. Barbuy & A. Renzini (Dordrecht: Kluwer), 225
Mas-Hesse, J. M., & Kunth, D. 1991, A&AS, 88, 399
Rice, W., Boulanger, F., Viallefond, F., Soifer, B. T., & Freedman, W. L. 1990, ApJ, 358, 418
Rosa, M., Joubert, M., & Benvenuti, P. 1984, A&AS, 57, 361
Schaller, G. Schaerer, D., Meynet, G., & Maeder, A. 1992, A&A, in press
Stecher, T. P., et al. 1992, ApJ, 395, L1
van den Bergh, S. 1991, PASP, 103, 609
Vílchez, J. M., Pagel, B. E. J., Díaz, A. I., Terlevich, E., & Edmunds, M. G., 1988, MNRAS, 235, 633.
Wilson, C. D., Freedman, W. L., & Madore, B. 1990, AJ, 99, 149